Dynamic elastic properties of brick masonry constituents

Nirvan Makoond*, Luca Pelà, Climent Molins

Department of Civil and Environmental Engineering, Universitat Politècnica de Catalunya (UPC-BarcelonaTech), Jordi Girona 1-3, 08034 Barcelona, Spain

Abstract

When subjected to dynamic loading, materials can exhibit a mechanical behaviour quite different from its static counterpart. The evaluation of dynamic properties is thus very useful in the assessment of existing masonry structures. This paper presents results of an experimental campaign to determine both the dynamic Young's modulus and the shear modulus of brick masonry constituents through two non-destructive testing methods. Following a discussion on the reliability of the methods, a robust procedure is described and tested on a variety of samples. The results show that the techniques can be successfully applied to provide reliable estimates of the dynamic elastic properties of brick masonry constituents.

1. Introduction

Static elastic properties of masonry constituents are in general well understood. Indeed, a considerable amount of information is available in literature on the determination and estimation of such properties. For instance, the European Committee for Standardisation (CEN) has approved a European Standard on the determination of the static elastic modulus for natural stone since 2005 [1]. Tests to determine static elastic properties rely mainly on measuring deformations while applying controlled loading. Hence, the modified application of recommendations from standards designed for other materials such as concrete is, at least in theory, relatively straightforward. As a consequence, several authors such as Binda et al. [2–5], Oliveira et al. [6–8] and Pelà et al. [9] have explored testing procedures to determine these properties for masonry constituents and assemblages. Many of these studies have shown that although the theory behind the evaluation of static elastic properties is well understood, the scatter of results in experimental studies remains high in many cases, often due to the difficulties related to measuring deformations in the elastic range of brittle materials such as those typically used as constituents in brick masonry constructions. Nevertheless, a considerable amount of information is still available, not only on best testing practices, but also on the range of expected results for different types of bricks and mortar, as well as on the effects which can influence the estimates of static elastic properties for brick masonry constituents.

Dynamic elastic properties refer to the constants that define a material's behaviour in the elastic range under vibratory conditions. When subjected to dynamic loading, experiments have shown that materials can feature a mechanical behaviour quite different from its static counterpart. A possible physical cause of this empirically known inequality between measured static and dynamic elastic moduli may be found in the different inelastic contributions to stress-strain which behave as a function of strain amplitude and frequency (energy and strain rate) [10]. Most of the studies available in literature focus on the relation between static and dynamic elastic properties of rocks in a geophysical context [11–14]. As such, although some authors, notably Totoev and Nichols [15, 16], have explored this relationship for specific types of bricks, it is still not

---

*Corresponding author

Email addresses:* `nirvan.makoond@upc.edu` (Nirvan Makoond), `luca.pela@upc.edu` (Luca Pelà), `climent.molins@upc.edu` (Climent Molins)

well understood.

The evaluation of elastic dynamic mechanical properties can prove to be very useful for the safety assessment of structures exposed to dynamic loading conditions. These properties can be calculated using data obtained from vibration tests or from the measured velocity of stress waves passing through the material. The American Society for Testing Materials (ASTM) approved two of the most relevant existing standards on test methods that can be used to evaluate these properties, namely:

- A standard on the evaluation of the dynamic Young's Modulus, Shear Modulus and Poisson's ratio by Impulse Excitation of Vibration (IEV) for homogeneous elastic materials [17].

- A standard for the determination of the propagation velocity of ultrasonic longitudinal stress waves through concrete which can be related to the material's dynamic elastic properties [18].

Since dynamic properties are not evaluated directly but computed based on assumptions derived from the known behaviour of materials under specific conditions, the application of recommendations from standards is not so straightforward, particularly when they have been designed for different materials. The parameters being measured (wave travel time, frequency of vibration) often rely on many conditions which need to be understood and controlled carefully. This operation is necessary to be able to use the expressions relating measured parameters to material constants.

The aforementioned work by Totoev and Nichols [15, 16] includes the evaluation of the dynamic Young's modulus for specific types of bricks. However, the range of experimental techniques as well as the range of different constituents tested is rather limited, particularly when compared to the information available on static properties. Notably, the dynamic Young's modulus was only evaluated through means of longitudinal vibration tests and traditional ultrasonic pulse velocity (UPV) testing with longitudinal stress waves (P-waves). In such studies, the dynamic Poisson's ratio is assumed as being invariant from the quasi-static one, and no procedure is described for the experimental determination of the dynamic Poisson's ratio or shear modulus through torsional vibration tests. Although this is most likely a reasonable assumption, there is not sufficient information available in literature for this relationship to be well-established. In fact, studies available in literature involving the determination of dynamic Poisson's ratio or shear moduli, such as [19] and [20], have only focused on very specific types of constituents. Moreover, although Totoev and Nichols [15, 16] mention that UPV measurements can provide information on the isotropy of bricks, no detailed information is provided on the validity or correct interpretation of P-wave travel time readings for anisotropic cases. In such cases, wave propagation is not necessarily governed by the same simplified laws as in isotropic media and therefore evaluation of the dynamic modulus of elasticity using P-wave velocities alone can be quite unreliable. Finally, in order to carry out the longitudinal vibration tests, the specimens are cut from whole bricks so that each resulting specimen has a greater ratio between the lateral dimensions and the length. Thus the non-destructive nature of the vibrational tests is not fully exploited.

The main aim of this research is to assess the applicability of a combined procedure based on two non-destructive techniques to experimentally determine both the dynamic Young's modulus and shear modulus of brick masonry constituents. The two chosen methods are UPV testing with P-waves and IEV testing. The theory behind these two methods, as well as the respective procedures for the estimation of the dynamic elastic properties, are described in Section 2. The two techniques were selected not only because of the simplicity and speed of their application, but also because they make use of equipment that is nowadays widely used in the construction industry and hence relatively accessible. UPV testing with P-wave transducers is commonly used for non-destructive quality control of concrete while accelerometers and data acquisition systems required for IEV testing are used for dynamic response testing and monitoring of many structures, such as bridges and towers. Moreover, the research also aims to test whole brick specimens since this would allow these methods to be applied to recently manufactured bricks as well as to those extracted from existing constructions. Mortar samples tested as part of this research were cast in moulds having dimensions of a standard brick ($290 \times 140 \times 40$ mm^3).

Different types of bricks and mortars were explored in order to derive useful ranges of results for different masonry typologies. Although an effort has been made to include specimens of varied quality and porosity in the sample set to appropriately validate testing protocols and analysis procedures, explicitly defining the relationship between porosity or chemical composition of the materials to the dynamic elastic properties is

2

beyond the scope of this research. Previous studies available in literature such as [21] and [22] address these relationships more directly for specific types of materials (alumina ceramics and specific stones).

As a result, a robust methodology, combining information from both UPV and IEV testing, for the determination of dynamic elastic properties of typical brick masonry constituents is proposed.

2. Background & theory

This section introduces the theory behind the two main testing techniques employed as part of this research. It highlights important concepts that are essential to the correct interpretation of results from IEV and UPV testing.

2.1. Impulse excitation of vibration (IEV) testing

It is known that specimens of elastic materials possess specific mechanical resonant frequencies that are determined by the elastic properties, mass, geometry of the test specimen and boundary conditions imposed by the test set-up. The dynamic elastic properties of a material can therefore be computed if the geometry, mass, and mechanical resonant frequencies of a suitable test specimen of that material can be measured. Test set-ups that isolate specific resonance modes together with the processing of recorded vibration signals, allow these resonant frequencies to be determined. Specifications on specimen dimensions, test set-ups, expressions relating identified resonant frequencies to dynamic properties as well as other considerations are described thoroughly in the Standard Test Method for Dynamic Young's Modulus, Shear Modulus, and Poissons Ratio by Impulse Excitation of Vibration released by ASTM [17].

The dynamic Young's modulus can be determined using the resonant frequency in either the flexural or the longitudinal mode of vibration. For the purpose of this study, the dynamic Young's modulus was only evaluated using the resonant frequency in the flexural mode because the ratios of dimensions of typical bricks means that the resonant frequency of the longitudinal mode would be much higher than that of the flexural mode. Since these frequencies were found to already be relatively high in the flexural mode, a quick estimate of the expected frequencies to be measured for the same Young's modulus in the longitudinal mode revealed that this frequency would fall outside the range that could be accurately measured by the data acquisition system. The dynamic shear modulus, or modulus of rigidity, is found using torsional resonant vibrations. To isolate the flexural mode of vibration, the ASTM standard [17] states that the rectangular specimen should be supported along the width at a distance of $(0.224 \times Length)$ from either end of the length, as shown in Figure 1(a). On the other hand, to isolate the torsional mode, the rectangular specimen should be supported along the midpoints across the width and length as shown in Figure 1(b). Figure 1 also shows the recommended impact and sensor locations for each test. An important recommendation from the ASTM standard [17] is to place any direct contact transducers along the nodal lines which ensures minimal interference with the free-vibration of the specimen.
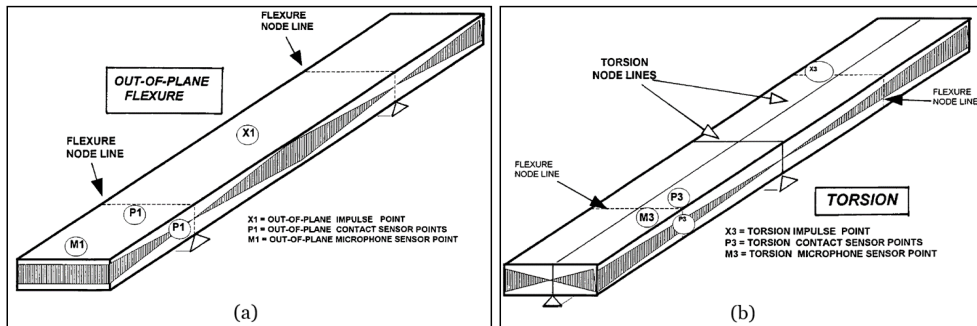

Figure 1: Impulse Excitation of Vibration: Specified test set-up, sensor and impact locations for the flexural mode(a) and torsional mode(b) according to [17].

For the fundamental flexure frequency of a rectangular bar, the dynamic Young's modulus can be evaluated using Equation (1), whilst for the fundamental torsional frequency, the dynamic shear modulus can be computed using Equation (2).

$$E = 0.9465\Big(\frac{m{f_f}^2}{b}\Big)\Big(\frac{L^3}{t^3}\Big)T_1 \tag{1}$$

3

$$G = \frac{4Lmf_t{}^2}{bt}[B/(1+A)] \tag{2}$$

Where E is the dynamic Young's modulus (Pa), m is the mass of the bar (g), b is the width of the bar (mm), L is the length of the bar (mm), t is the thickness of the bar (mm), f_f is the resonant frequency in flexure (Hz), T_1 is a correction factor dependent on Poisson's ratio as well as t and L, G is the dynamic shear modulus (Pa), f_t is the resonant frequency in torsion (Hz), B and A are correction factors dependent on b and t.

As we can see from Equation (2), the computation of the dynamic shear modulus from the measured torsional resonant frequency does not require knowledge of the dynamic Poisson's ratio. However, this unknown parameter is required for the evaluation of the T1 parameter in Equation (1). If isotropy is assumed, there exists a well known relationship between the Poisson's ratio, the Young's modulus and the shear modulus. Hence, for the isotropic case, the iterative procedure shown in Figure 2 can be used to find a suitable Poisson's ratio that will satisfy this relationship. In order for the iterative procedure to converge, a reasonable initial Poisson's ratio (ν_0) has to be selected. For all the specimens tested as part of this research, a ν_0 of 0.2 proved to be a good initial value to attain convergence.
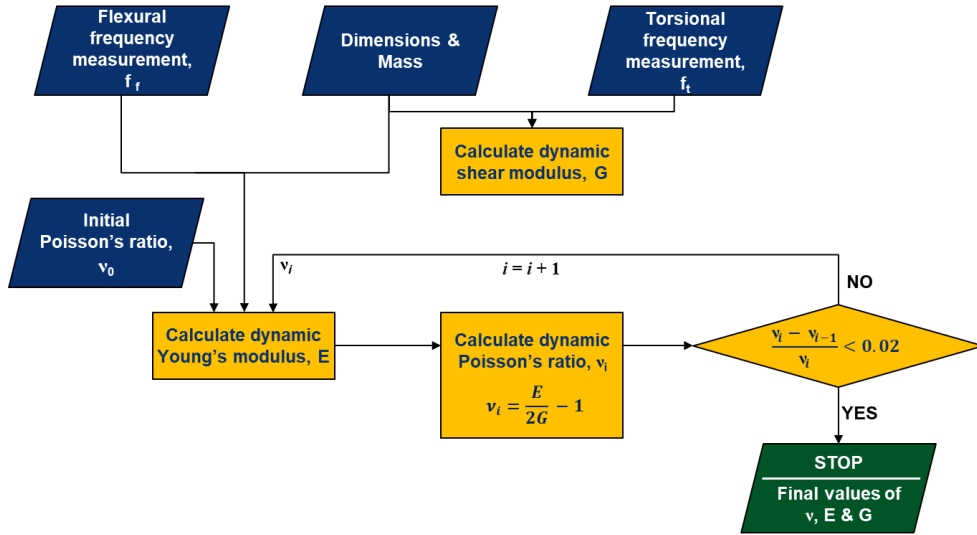

Figure 2: Impulse Excitation of Vibration: Procedure for estimating dynamic Young's modulus, shear modulus and Poisson's ratio according to [17].

2.2. Ultrasonic pulse velocity (UPV) testing

Research on wave propagation in elastic solid materials dates back to the early 19th century [23]. UPV testing makes use of elastic (or acoustic) waves which are in fact mechanical vibrations that propagate in gases, liquids and solids. Ultrasound corresponds to mechanical waves propagating at frequencies above the range of human hearing (conventionally 20 kHz) [24].

Although many different patterns of vibrational motion exist at the atomic level, in solids it can be said that two modes of bulk wave propagation exist that are most relevant to ultrasonic testing in the context of this research, namely:

- **Longitudinal waves:** Waves with particle displacement in the direction of wave propagation. These waves travel the fastest and are also known as compression waves or P-waves. The most accessible and commonly used electro-acoustical transducers in the construction industry produce waves primarily of this type [25].

- **Shear waves:** Also known as transverse waves, the direction of vibrations in these waves is normal to the direction of wave propagation [26]. Note that the direction of particle vibration is referred to as the polarization.

2.2.1. Wave propagation in isotropic media

The micro-structure of many engineering materials is formed from many randomly oriented grains which results in the mechanical properties being independent of direction on the macroscopic scale. These materials are therefore isotropic. In the case of ultrasonic wave propagation, when the ultrasonic wavelength is much greater than the grain size, isotropic assumptions are quite valid [27]. Under these circumstances, bulk waves propagate with equal velocity in every direction. Hence, in an infinite[i] isotropic material, wave energy may only propagate in two modes: longitudinal or shear. The equation of motion for an elastic isotropic solid can be decomposed into the following two wave equations relating the velocity of propagation of a longitudinal wave (c_l) and of a shear wave (c_s) to the material density ρ and the two constants used in Hooke's law for an elastic isotropic material (Young's Modulus E and Poisson's ratio ν) [27, 29].

$$c_l = \left(\frac{E(1-\nu)}{\rho(1+\nu)(1-2\nu)} \right)^{\frac{1}{2}} \tag{3}$$

$$c_s = \left(\frac{E}{2\rho(1+\nu)} \right)^{\frac{1}{2}} \tag{4}$$

However, if a wave encounters a boundary separating two media with different properties, part of the disturbance is reflected and part is transmitted into the second medium [23]. Similarly, if a body has a finite cross-section which is comparable to the wavelength of the disturbance, waves can bounce back and forth between the bounding surfaces. Such circumstances can significantly increase the complexity of analysing the recorded wave signals and relating dynamic elastic properties of the material to travel time measurements. This extra layer of complexity can be avoided by selecting the frequency of the signal generated by the ultrasonic transducer, as described in detail in Section 3.3.1.

2.2.2. Standard test methods

As previously mentioned, UPV testing in the construction industry has traditionally been limited to P-wave measurements mainly used for inspection and quality control. As such, the most relevant standards for the purpose of this investigation only cover determination of the propagation velocity of ultrasonic longitudinal waves in hardened concrete (EN 12504-4:2004 [30] and ASTM C597 [18]). Although the ASTM standard presents the relationship shown in Equation (3), it clearly states that the method should not be considered an adequate test for establishing compliance of the modulus of elasticity of field concrete with that assumed in the design. One of the reasons for this is that the relationship described in Equation (3) requires knowledge of the dynamic Poisson's ratio to determine the dynamic Young's modulus from the pulse velocity. Since the ASTM C597 standard is concerned only with determination of the velocity, it provides no indication of how to determine the Poisson's ratio.

The standard test method makes use of a pulse generator, a pair of electro-acoustical transducers, an amplifier, a time measuring circuit and a time display unit as shown in Figure 3.
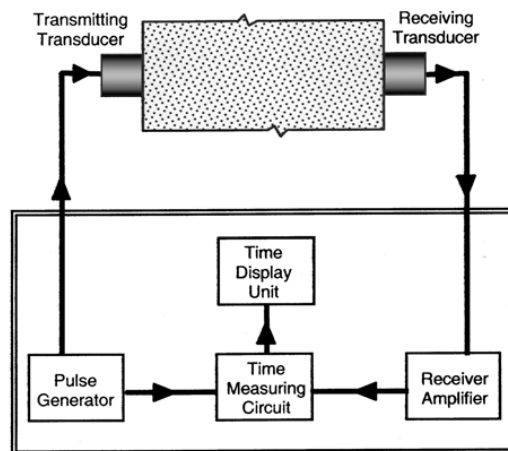

Figure 3: Ultrasonic Pulse Velocity: Test set-up according to ASTM C597 [18]

---

[i]Note that in this context, infinite media means that boundaries have no influence on wave propagation [28].

It is stated that for best results, the transducers should be located directly opposite each other. The distance between centres of transducer faces must be measured, and the pulse velocity can then be calculated by dividing this distance by the pulse transit time measured using the apparatus as shown in Figure 3.

2.2.3. Wave propagation in anisotropic media

Previous research indicates that bricks formed by extrusion can exhibit a significant level of anisotropy [31]. Wave propagation in anisotropic media is substantially different from the isotropic case. The most significant difference is that elastic waves propagate with a velocity that depends on direction [27]. Moreover, the number of independent constants which define the elastic behaviour of the material itself will be greater than 2 and will depend on the symmetry class or type of anisotropy assumed. Assuming an orthotropic material will result in 9 independent elastic constants while assuming transverse isotropy (material with a plane of isotropy) will result in 5. Furthermore, unlike the isotropic case, the wave modes are not necessarily pure modes as the particle vibration is neither parallel nor perpendicular to the propagation direction [27]. In practice however, the anisotropic modes do show similarities to the isotropic modes and in these cases are referred to as quasi-longitudinal and quasi-shear. The quasi-shear modes are distinguished further by whether they are primarily horizontally (SH-waves) or vertically (SV-waves) polarized.

Christoffel's equations can be used to relate measured ultrasonic pulse velocities to the elastic constants. These expressions and related experimental procedures are not discussed here but a thorough description is given in [29]. However, because the propagation of a wave along a specific plane does not depend on all the elastic constants used in the material definition, the experimental procedure has to include measurements across different planes. Moreover, the velocities of three wave modes (P-waves, SH-waves and SV-waves) need to be measured across each of these planes in order to determine the elastic constants. Hence, the full elastic characterisation of an anisotropic material cannot be directly determined using P-wave velocity measurements alone.
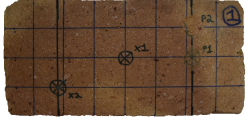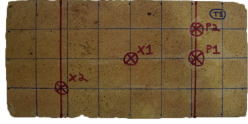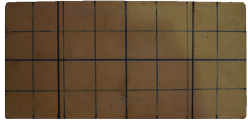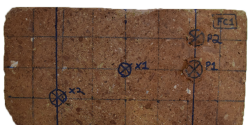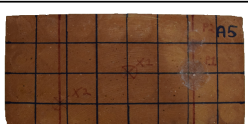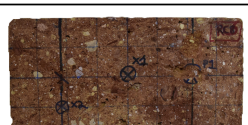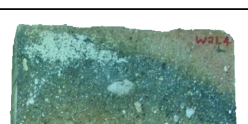
3. Experimental program

The experimental campaign was carried out at the Laboratory of Technology of Structures and Building Materials of the Universitat Politècnica de Catalunya (UPC-BarcelonaTech). This section presents information about the material components, the preparation of the specimens and the testing procedures.

3.1. Materials tested

7 different groups of solid bricks were tested in order to investigate different types of materials, both used in existing and new constructions. 5 of these groups (I(a), I(b), III, V(a) and V(b)) consisted of handmade bricks formed by moulding. Of these, 2 groups (I(a) and I(b)) consisted of solid terracotta bricks, tested after production, before use in any construction project. On the other hand, group III bricks have been extracted from an industrial complex built in the early 20th Century, part of Barcelona's industrial heritage. Bricks from group V(a) and V(b) were extracted from a typical residential building located in Rambla de Catalunya, a street in the centre of Barcelona. It should be noted that the UPV testing procedure for specimens from group V(b) consisted of less measurements (more detail is given in Section 3.3.3). The 2 groups of solid bricks manufactured using a conventional extrusion process (II and IV) were both tested before use in any construction project. The type of bricks from group II have been used to build timbrel vaults in an ongoing construction project in Barcelona. Finally, bricks from group IV are manufactured using an automated process and are compliant with the EN 771-1:2011 standard [32]. A brief summary of the different groups tested is given in Table 1.

Table 1: Groups of brick types tested.

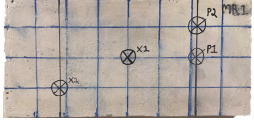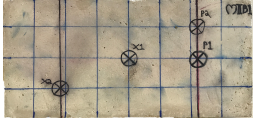| Group	Specimen labels	Manufacturing	Year	f_{cn}* [MPa]	Avg. Mass [g]	Average measured dimensions [mm³]	Sample view
I(a)	**1 - 7**	Handmade in moulds	2017	17.4	3,212	40 × 147 × 306	
I(b)	**T1 - T6**	Handmade in moulds	2015	17.4[†]	3,136	40 × 146 × 306	
II	**SF1 - SF5**	Conventional extrusion	2016	40.0	2,549	38 × 141 × 291	
III	**FC1 - FC3**	Handmade in moulds	1903	18.8	2,900	43 × 144 × 294	
IV	**A1 - A6**	Conventional extrusion	2018	52.7	2,423	40 × 132 × 272	
V(a)	**RC6,RC8**	Handmade in moulds	1930	10.7[‡]	2,907	40 × 145 × 291	
V(b)	**W2L1 - W2L5, W2L7**	Handmade in moulds	1930	10.7	3,134	43 × 145 × 294	

* Reference normalised compressive strength for corresponding brick type obtained by testing bricks in accordance with the European standard EN 772-1 [33].

† Same reference normalised compressive strength shown as bricks from group I(a). Bricks from group I(b) were produced with the same raw materials and using the same manufacturing technique as bricks from group I(a).

‡ Same reference normalised compressive strength shown as bricks from group V(b). Bricks from group V(a) were extracted from the same wall as bricks from group V(b).

Two different types of mortar, which can be considered as being at either end of the range of stiffness encountered in brick masonry structures, were prepared and tested, i.e. a weakened hydraulic lime mortar (MB and MIIB specimen groups) and a cement mortar (MC). The M5 hydraulic lime was weakened by the addition of an inert limestone filler so that it would be more representative of weaker mortars found in historical constructions. Specimens from group MB were uncast after 5 days and tested after 28 days since initial casting. Since specimens from group MB were found to be still relatively fragile at the time of uncasting, MIIB mortar specimens were uncast after 14 days. These specimens were also tested 28 days after initial casting. Finally, the cement mortar specimens were uncast after 1 day and tested 14 days after casting. Table 2 provides a summary of the most important characteristics of the different mortar specimen groups tested.

Table 2: Groups of mortar types tested.

Group	Specimen labels	Mix proportions	f_{cn}* (28 days) [MPa]	Avg. Mass [g]	Average measured dimensions [mm³]	Sample view
MB	MB1 - MB5	Lime : filler : water 1 : 0.64 : 0.37	2.3	2,930	$41 \times 139 \times 290$	
MIIB	MIIB1 - MIIB8	Lime : filler : water 1 : 0.64 : 0.37	2.0	3,237	$42 \times 139 \times 290$	
MC	MC1 - MC5	Cement : sand : water 1 : 3 : 0.5	49.3	3,632	$41 \times 139 \times 291$	

* Reference normalised compressive strength for corresponding mortar type obtained by testing prismatic specimens in accordance with the European standard EN 1015-11 [34].

3.2. Impulse excitation of vibration testing

3.2.1. Testing equipment

For each IEV test, a suitable data acquisition system able to record the vibrations of the specimen was required so that the resonant frequency could then be extracted from the resulting acceleration-time history. The data acquisition system designed for these tests consisted of a lightweight (25 g) triaxial integrated circuit piezoelectric accelerometer, a signal conditioner (PCB 482A16) and an embedded real-time controller (cRIO-9064) equipped with a vibration input module (NI-9234). During testing, the real-time controller was connected to a laptop equipped with a program specifically created for these acquisitions using the LabVIEW 2016 programming environment from National Instruments [35].

3.2.2. Specimen preparation

It is clear from Equation (1) that the accuracy of the estimated dynamic elastic modulus is highly dependent on the regularity of the specimen and the uncertainty related to its dimensions. For instance, since the thickness and length variables in the modulus equation have an exponent of 3, an error of 1% in these dimensions would result in an error of 3% in the estimated modulus. Hence, in order to reduce the variations in dimensions within each specimen, the surfaces of brick specimens were polished in order to regularise the faces.

It is important to note that moisture content of the specimens can have an effect on the observed resonant frequency and hence on the estimated dynamic elastic properties. In order to control this parameter, all specimens were dried at 120 °C in a drying oven until the mass was constant as recommended in [36] before the execution of any tests.

Preparation of specimens also entailed marking the lines along which each specimen should be supported during testing to isolate the fundamental flexural and torsional modes. Finally, the impact and sensor locations were also marked as shown in Figure 4 in order to facilitate mounting of the sensor and ensure consistent impulse excitations.
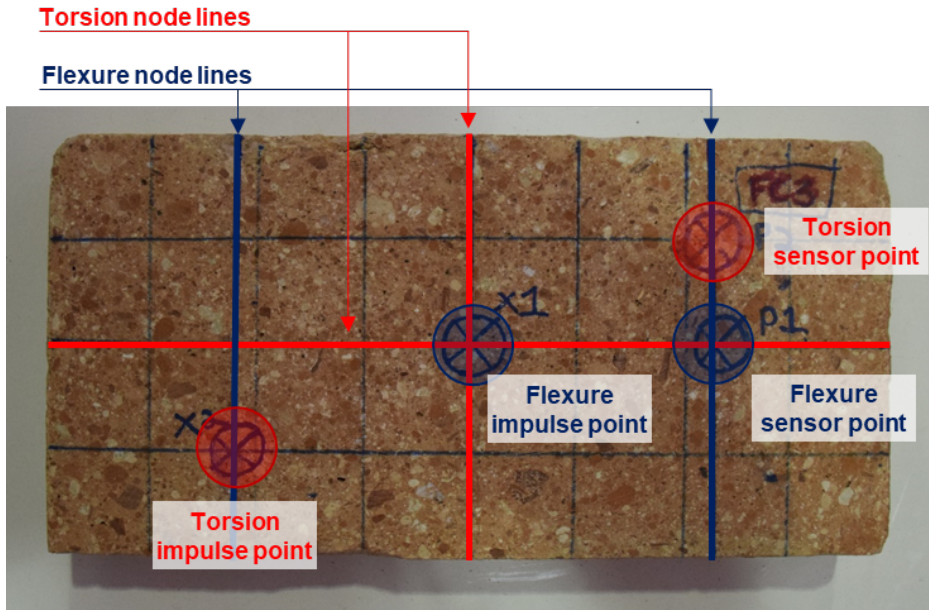
Figure 4: Markings made on every specimen prior to IEV testing.

3.2.3. Test set-up

Simple custom rigid supports were fabricated in order to isolate the flexural and torsional modes. For all tests, the supports were placed on isolation pads in order to prevent ambient vibrations from being picked up by the accelerometer. The supports were metallic and had a sharp edge in contact with the specimen along the nodal lines. The supports can be seen in Figure 5 which also shows the test set-ups used for flexural (a) and torsional (b) IEV tests on whole bricks.
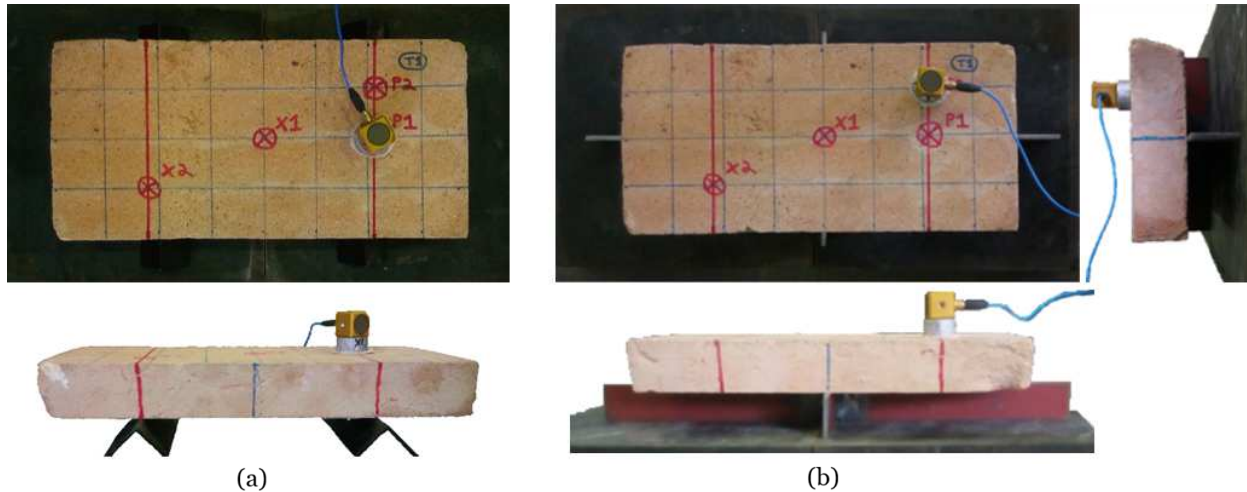

(a)　　　　　　　　　　　　　　　　　(b)

Figure 5: (a) Test set-up for flexural IEV test (view from top and front). (b) Test set-up for torsional IEV test (view from top, front and side).

For all tests on bricks, the accelerometer was fixed using an adhesive mounting technique via a lightweight (18 g) aluminium mounting plate fixed to the brick's surface using a 2-component cold curing superglue. This ensured adequate vibration transmissibility while also reducing any mass loading effects (see Figure 5). Although this technique proved to impart very little damage on most bricks, removal of the mounting plate did cause some loss of material from the surface of many bricks. This loss of material proved to be quite significant in the case of the fragile MB Mortars. Since one of the secondary aims of this research campaign is to keep the specimens as intact as possible for further testing, a less intrusive mounting method was desirable, particularly for the more fragile lime mortar specimens. Hence, a different mounting technique was tested which involved fixing the accelerometer on the surface of the specimen using scrim-backed adhesive tape as shown in Figure 6. Naturally, this technique further reduces any mass loading effects since the mass of

the adhesive tape is much lower than that of the mounting plate. However, since it is a less commonly used mounting technique than the aforementioned one, the adequacy of its vibration transmissibility had to be verified for the purpose of these tests. In order to achieve this, a comparative study was carried out between the two mounting methods on all the specimens from the MB mortar group. The observed resonant frequency was found to differ by less than 1.2% across all the specimens. Hence, the mounting technique with the scrim-backed adhesive tape was used to test all mortar specimens to avoid any further damage to the specimens.
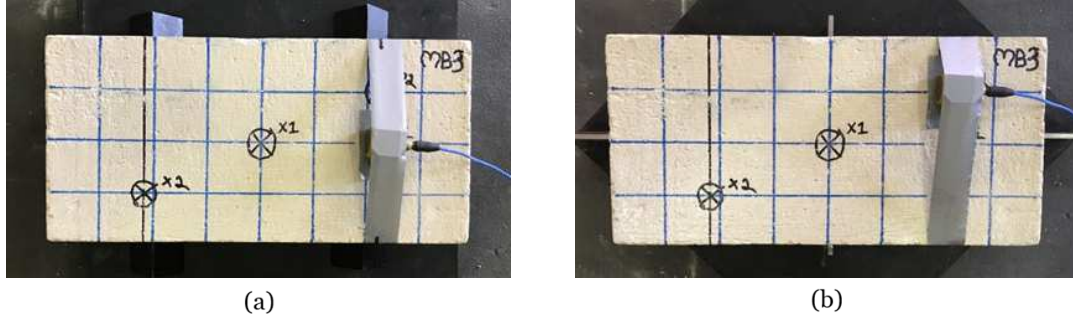

Figure 6: Accelerometer mounting using scrim-backed adhesive tape for (a) flexural test set-up and (b) torsional test set-up of IEV tests.

Another important consideration before testing any specimens involves selecting an appropriate sampling frequency to be used for all the tests. Based on the capabilities of every element of the data acquisition system, a sufficiently high sampling frequency must be chosen to prevent any aliasing. This requires an estimation of the expected resonant frequencies that need to be measured. In the case of the specimens tested for this research campaign, the observed resonant frequencies varied from 586 Hz to 1794 Hz for the flexural tests and from 746 Hz to 2099 Hz for the torsional tests. A sampling frequency of 20 kHz was used for all the IEV tests.

3.2.4. Testing procedure

Before actually executing the vibration tests, the mass and dimensions of each specimen had to be determined accurately for consequent computation of the dynamic elastic properties. The mass was determined using an electronic balance with a precision of 0.5 g, satisfying the 0.1% of specimen mass requirement stipulated in the ASTM standard [17] for all specimens tested. Each dimension was taken as the average of multiple readings along each of them at the locations shown in Figure 7. These measurements were taken with a Vernier caliper with a precision of 0.02 mm. The multiple measurements were not only used to compute the average dimensions but also to quantify the variation in dimensions of the specimens. The coefficients of variation of all dimensions of all specimens were found to be less than 2% except for 6 specimens which had coefficients of variations of less than 4% for the measured thickness dimensions.
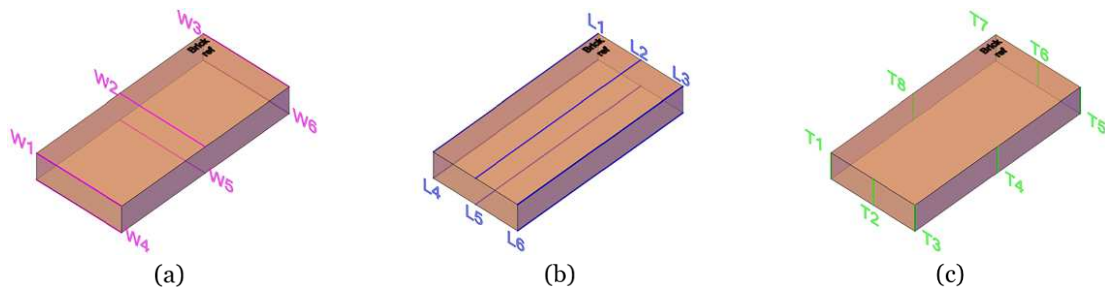
Figure 7: Locations of the 20 measurements taken with a Vernier caliper for every specimen tested under IEV. (a) 6 measurements of the length taken for every specimen. (b) 6 measurements of the width taken for every specimen. (c) 8 measurements of the thickness taken for every specimen.

Once the set-ups described in the previous section have been prepared, the IEV tests simply involve applying an impulse at the specified location using an impact tool which satisfies the requirements stated in [17]. In practice, the size and geometry of the tool depends on the size and weight of the specimen and the force needed to produce vibration. In the case of the bricks, one of the most important considerations

10

was to ensure that the impact was not too strong for the higher amplitudes of the recorded signals not to fall outside the measurable range of the accelerometer (±5 g).

For each IEV test, the vibration signals were recorded whilst the specimen was impacted several times (see Figure 8). An appropriate feature extraction procedure needed to be implemented in order to extract the resonant frequency from the acceleration-time histories. It should be noted that one of the requirements from the ASTM standard [17] is to determine the resonant frequency as the average of five consecutive readings which lie within 1% of each other. Because of this requirement, it was essential to be able to estimate the resonant frequency during testing itself. Hence, the Frequency Domain Decomposition (FDD) technique was used, because it does not only allow fast estimation of the resonant frequency but also exploits the data recorded from the 3 channels of the tri-axial accelerometer for improved accuracy. A custom script for processing the files generated by the LabVIEW acquisition program and subsequently carrying out FDD analysis was created in the MATLAB® computing environment [37] by modifying the original FDD script by [38]. This process is summarised in Figure 8.
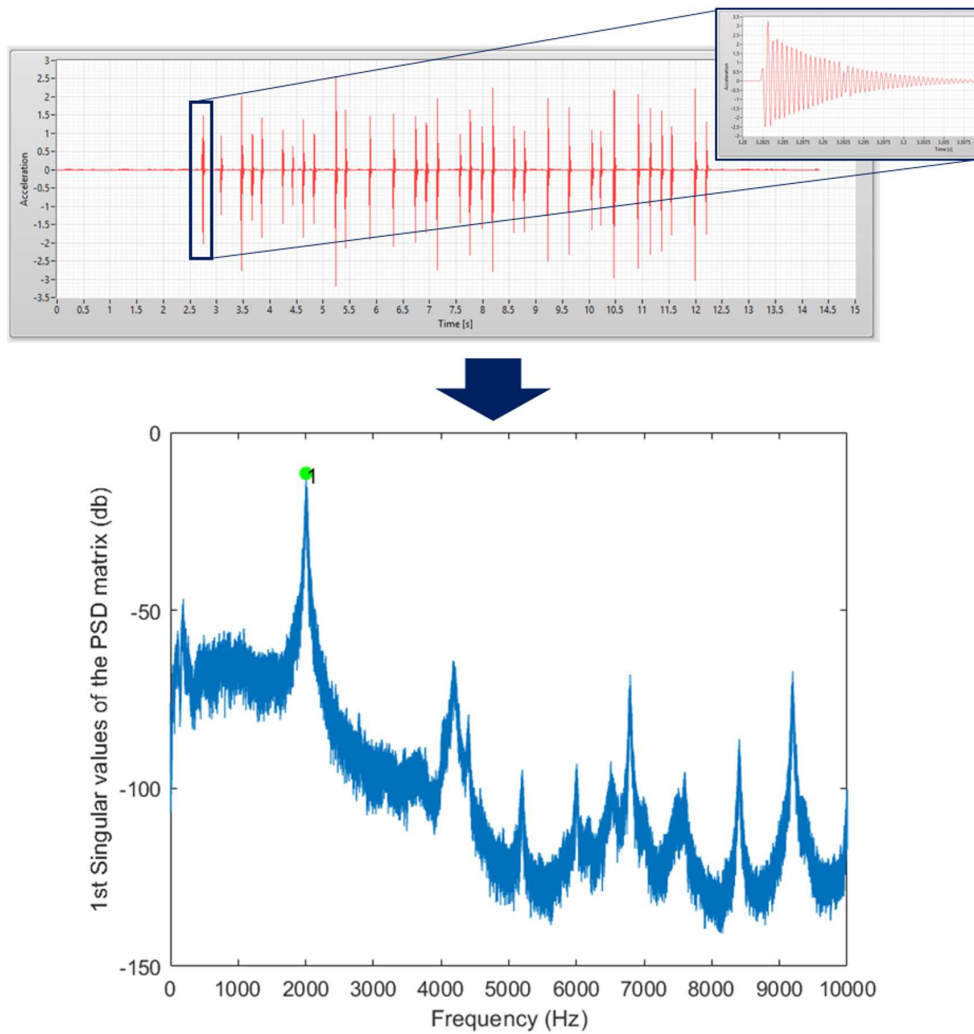
Figure 8: Top: Acceleration-time history for a single IEV test (with a zoom-in of a single impulse shown). Bottom: Selection of peak during FDD process.

Once the resonant frequencies were extracted, Equations (1) and (2) could be used to estimate the dynamic Young's modulus and shear modulus respectively. The iterative procedure described in Section 2.1 was used to estimate the dynamic Poisson's ratio and update the dynamic Young's modulus accordingly.

11

3.3. Ultrasonic pulse velocity testing

3.3.1. Testing equipment

The ultrasonic pulse travel times were recorded using a PROCEQ Pundit® PL-200 [39] commercial ultrasonic testing instrument. This equipment incorporates a pulse generator, receiver amplifier and time measuring circuit into one unit with a touch-screen display that can be used to view the waveform of recorded signals and pulse travel time in real-time. Different transducers can be used with this instrument, each of which is better suited for different applications.

The selection of the appropriate transducer is largely dependent on grain size and on the dimensions of the test object. The frequency of the transducer should be chosen so that the resulting ultrasonic pulse has a wavelength smaller than the minimum lateral dimension of the test specimen but at least twice as large as the grain size [39]. Since the wavelength is dependent on the velocity of propagation (wavelength equals velocity divided by frequency), the selection of an appropriate transducer before testing the material is not so straightforward. It is known that the ultrasonic pulse velocity in concrete ranges from 3000 m/s to 5000 m/s [39]. Most materials tested as part of this campaign are characterised by lower velocities. In fact, the observed velocities vary from 1132 m/s (Type V(b) brick) to 4270 m/s (CM Mortar). A pair of 250 kHz transducers was used for all the UPV tests carried out as part of this research, resulting in wavelengths ranging from 5 mm to 17 mm. These wavelengths are all smaller than 38 mm, the smallest thickness encountered across all specimens. Although this range of wavelengths can also be considered as being greater than the average grain size of the materials under test, in some cases, the specimens contained significant heterogeneities such as voids or aggregates that are larger than the aforementioned wavelength range. Moreover, the specimens characterised by lower ultrasonic pulse velocities also turn out to be the most heterogeneous. This results in a greater likelihood of scattering affecting the reliability of the results for these specimens, since the wavelengths of the ultrasonic pulses are smaller while the effective grain size can be considered as being larger due to the heterogeneities. Taking multiple readings at different locations can help to improve the reliability of results in such cases.

3.3.2. Treatment of specimens

Besides using a coupling gel between the transducers and the material during testing, the surfaces of the bricks were polished beforehand to ensure a smooth surface and hence prevent excessive loss of signal due to inadequate acoustic coupling. Since all the mortar specimens were cast in specifically designed moulds, their surfaces were adequately smooth and no further polishing was carried out.

As is the case for IEV tests, moisture content of the specimens is another factor that can influence UPV results. Hence, to control this parameter, all measurements were made on oven-dried specimens which had been allowed to stabilise to room temperature.

The final preparation step before executing the UPV tests involved marking the locations through which the velocity will be measured in order to be able to accurately position the transducers and measure the corresponding path lengths. A 4×8 grid of equal divisions on the largest faces of each specimen was used to locate all path lengths across the length, width and thickness (see Figure 4).

3.3.3. Testing procedure

Before any UPV tests were carried out, the mass and dimensions measured for the IEV tests were used to compute the density of the specimen which is required to evaluate the dynamic Young's modulus using Equation (3).

All measurements of pulse transit times were carried out using direct transmission with the transducers arranged directly opposite each other, widely considered as the optimum configuration for accurate pulse velocity determination. Using the UPV evaluated in this way into Equation (3) can be considered as giving a very localised estimate of the elastic properties since the velocity is only representative of the path along which the pulse travelled. Since it is known that many types of brick masonry constituents can have a significant level of heterogeneity, and even anisotropy in some cases, it is important to determine the pulse velocity at multiple locations and even across different directions before utilising them to evaluate the elastic constants describing the overall material behaviour. For the purpose of this research, three different variables were defined to describe the elastic moduli computed from multiple pulse velocities evaluated across the three different directions of each brick-sized specimen (length, width and thickness). They will hereafter

12

be referred to as $E_{UPV,L}$, $E_{UPV,W}$ and $E_{UPV,T}$.

For the UPV tests across the length and width of specimens, the reported pulse transit time at a single location was taken as the average of five consecutive readings with a coefficient of variation of less than 2% to reduce the effect of any measurement errors. The pulse transit time was measured at 3 locations across the length as shown in Figure 9 and 3 locations across the width as shown in Figure 10. The path lengths at these locations were measured using a Vernier caliper and the pulse velocity was computed by dividing the path length by the transit time. $E_{UPV,L}$ was then computed from Equation (3) using the average of the computed velocities from the 3 length locations specified and the Poisson's ratio estimated from the IEV tests. $E_{UPV,W}$ was computed using exactly the same procedure but using the velocities computed from the transit times and path lengths measured across the width.
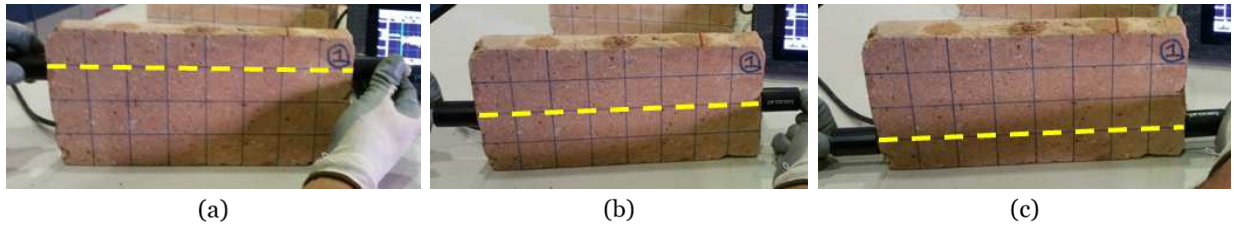

Figure 9: Locations of ultrasonic pulse travel time measurements across length: (a) Top quarter, (b) Middle, (c) Bottom quarter.
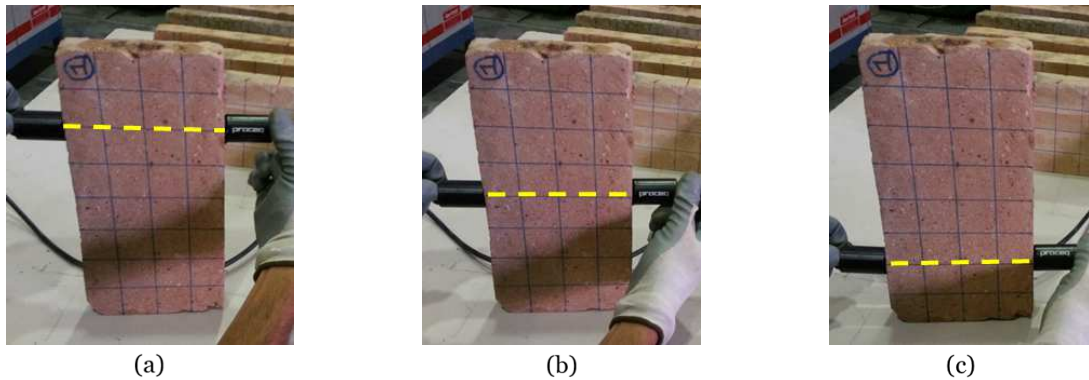

Figure 10: Locations of ultrasonic pulse travel time measurements across width: (a) Top quarter, (b) Middle, (c) Bottom quarter

Specimens from group V(b) were tested before the methodology described herein had been developed. As such, for specimens from group V(b), the transit time was only measured at the middle location across the length and the width. Moreover, no measurements of pulse transit times were taken across the thickness of specimens from this group.

For all other specimens, the procedure used for computing $E_{UPV,T}$ differed from that used for $E_{UPV,L}$ and $E_{UPV,W}$. Due to the shorter distance of the path length, it was expected that the effect of heterogeneities and scattering would be more significant. As such, the pulse transit time across the thickness was measured at 32 different locations on the face of each specimen as shown in Figure 11. The 32 measurements were used to generate travel time contour maps which could also be used to assess the heterogeneity of each specimen. In order to minimise the effect of any measurement errors, two consecutive sets of 32 readings were taken for each specimen and corresponding readings that differed by more than 2% were eliminated from any further computation. Since taking 32 measurements of path length was both time-consuming and impractical (parts at the centre of specimens were difficult to access to measure accurately), the pulse velocity was computed by dividing the average of the 8 thickness measurements taken as part of the IEV procedure by the average of the 32 measurements of pulse transit times. $E_{UPV,T}$ was then computed for each specimen from this computed velocity and using the Poisson's ratio estimated from IEV testing.
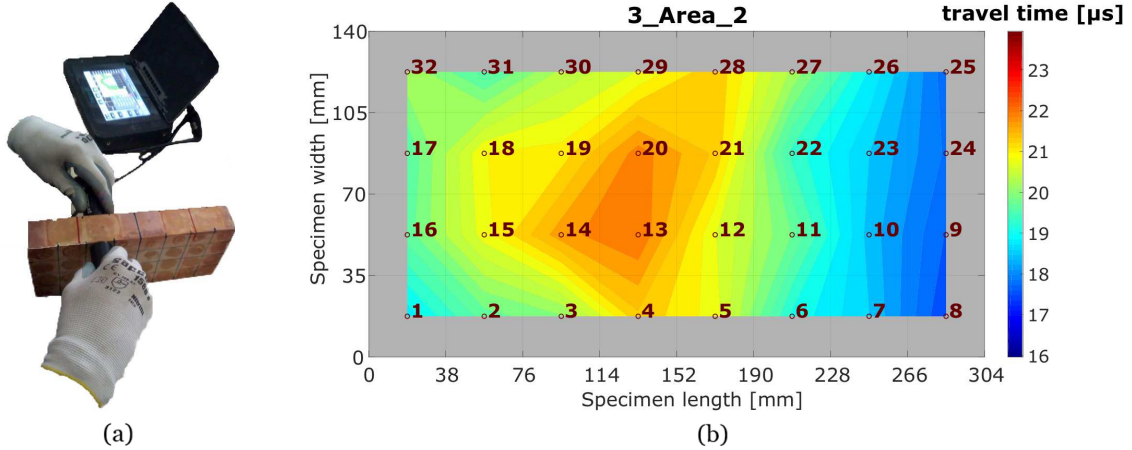
Figure 11: (a) Measurement of ultrasonic pulse transit time across thickness. (b) Example of an ultrasonic travel time colour map generated from 32 measurements over the face of each specimen.

4. Results and discussion

As described in Section 2.1, the dynamic Young's modulus (E_{IEV}), shear modulus (G_{IEV}) and Poisson's ratio (ν_{IEV}) for each specimen were computed from the measured mass, dimensions and fundamental frequencies by direct application of Equations (1) and (2) through the procedure described in Figure 2. The average of these results for each specimen group are presented in Table 3.

Table 3: Final estimated dynamic elastic properties from IEV testing.

Specimen Group	No. of specimens tested	Average values					
		E_{IEV} [MPa]	coeff. of variation	G_{IEV} [MPa]	coeff. of variation	ν_{IEV} [MPa]	coeff. of variation
35		**Units**					
I(a)	7	7,882	15%	3,530	15%	0.12	14%
I(b)	6	7,931	17%	3,628	17%	0.09	41%
II	5	18,313	1%	7,240	1%	0.26	7%
III	3	7,107	13%	3,309	10%	0.07	31%
IV	6	15,505	1%	5,733	1%	0.35	5%
V(a)	2	5,475	8%	2,525	5%	0.08	31%
V(b)	6	4,068	30%	1,965	29%	0.03	70%
21		**Mortar**					
MB	5	3,987	10%	1,811	9%	0.10	16%
MIIB	8	4,269	6%	1,886	6%	0.12	24%
MC	8	28,954	5%	11,417	3%	0.27	8%

As can be expected, in the case of bricks, the specimens produced by extrusion (groups II and IV) have higher values of dynamic Young's and shear moduli. This is because they are generally of higher quality and less porous than the bricks handmade in moulds and therefore exhibit a more stiff elastic behaviour. Similarly, the more modern cement mortar specimens appear to be much more stiff than the weaker lime mortars.

In addition to the estimates of the dynamic properties from IEV tests, dynamic Young's moduli for every specimen were also computed using Equation (3) from the average ultrasonic pulse velocity across different directions, derived as described in Section 3.3. This results in three estimates of the dynamic Young's modulus from UPV tests for every specimen, corresponding to its three main dimensions ($E_{UPV,L}$, $E_{UPV,W}$ and $E_{UPV,T}$). The average of these results for each specimen group are presented in Table 4.

14

Table 4: Estimated dynamic Young's modulus from UPV measurements across different directions.

Specimen Group	No. of specimens tested	Average values					
		$E_{UPV,L}$ [MPa]	coeff. of variation	$E_{UPV,W}$ [MPa]	coeff. of variation	$E_{UPV,T}$ [MPa]	coeff. of variation
	35	Units					
I(a)	7	7,837	18%	8,241	19%	5,764	20%
I(b)	6	7,938	13%	8,189	15%	5,979	17%
II	5	13,756	4%	15,199	4%	8,924	5%
III	3	7,305	2%	8,717	7%	8,016	15%
IV	6	9,157	8%	7,109	8%	12,035	8%
V(a)	2	5,498	4%	6,336	7%	5,754	14%
V(b)	6	4,604	35%	5,538	22%	-	-
	21	Mortar					
MB	5	4,527	6%	5,686	7%	6,230	7%
MIIB	8	4,887	16%	6,486	4%	6,123	2%
MC	8	28,601	4%	30,125	6%	29,236	4%

One of the most useful applications of the estimated dynamic Young's moduli across different directions is to evaluate if the specimens are actually isotropic. As such, a comparison of the relative scatters between these estimated properties for every specimen group is summarised in Table 5. The scatters are normalised to $E_{UPV,L}$ which can be considered the most reliable estimate from UPV tests carried out as part of this research. This is due to the fact that it is computed from the pulse velocity determined across the largest dimension of the specimens, hence minimising the effects of localised heterogeneities as well as those of measurement errors.

As described in Section 3.3.3, the 32 measurements of pulse transit time across the thickness cover almost the whole area over the two largest opposing faces of each specimen. Hence, for each set of readings, the maximum variation of the pulse transit times measured across the thickness ($\Delta t_T = t_{T,max} - t_{T,min}$) can provide an indication of the level of heterogeneity for each specimen. As mentioned in Section 3.3.3, two consecutive sets of readings were taken for each specimen. Therefore the representative maximum variation of each specimen ($\Delta t_{T,spec}$) was taken as the average of $\Delta t_{T,1}$ and $\Delta t_{T,2}$. Similarly, the representative average measured pulse transit time of each specimen ($\overline{t_{T,spec}}$) was taken as the average of $\overline{t_{T,1}}$ and $\overline{t_{T,2}}$. In order to allow adequate comparisons between specimens, a unitless heterogeneity measure for each specimen (HM_{spec}) was computed as follows:

$$HM_{spec} = \frac{\Delta t_{T,spec}}{\overline{t_{T,spec}}} \qquad (5)$$

Subsequently, the heterogeneity measure for a specimen group (HM_{Group}) was computed as the average of the HM_{spec} values of all specimens belonging to that group. These values are presented in the last column of Table 5.

Table 5: Comparison of dynamic Young's modulus from UPV measurements across different directions and heterogeneity measure for each specimen group.

Specimen Group	No. of specimens tested	Average values			HM_{Group}
		$\frac{E_{UPV,L}-E_{UPV,W}}{E_{UPV,L}}$	$\frac{E_{UPV,L}-E_{UPV,T}}{E_{UPV,L}}$	$\frac{E_{UPV,W}-E_{UPV,T}}{E_{UPV,L}}$	
	35	Units			
I(a)	7	-5%	26%	32%	**24%**
I(b)	6	-3%	25%	28%	**22%**
II	5	-10%	**35%**	**46%**	10%
III	3	-19%	-10%	10%	**26%**
IV	6	22%	**-31%**	**-54%**	8%
V(a)	2	-15%	-5%	11%	**26%**
V(b)	6	-20%	-	-	-
	21	Mortar			
MB	5	-26%	-38%	-12%	16%
MIIB	8	-33%	-25%	7%	11%
MC	8	-5%	-2%	3%	9%

15

The comparisons in Table 5 reveal that the bricks produced by extrusion (groups II and IV) display a higher level of anisotropy since the relative scatters between estimated dynamic Young's moduli for different directions were consistently greater for specimens from these two groups. It should be noted that the average values of the relative scatters between the estimated dynamic Young's moduli for specific directions also appear to be significant for some of the other specimen groups tested (I(a), I(b), MB, MIIB). However, there are much greater variations in these relative scatters among individual specimens from these groups when compared to the variations among the specimens from groups II and IV. This can be expected due to the greater homogeneity of the bricks manufactured by extrusion, confirmed by the significantly lower group heterogeneity measures (see Table 5). It is clear to see that although the comparison of estimated dynamic Young's moduli from ultrasonic P-wave velocities in different directions can provide some information on the inherent anisotropy of the material, it can be misleading and hence requires very careful interpretation. Moreover, as described in Section 2.2.3, the wave modes are not necessarily pure modes in anisotropic media. Therefore, the ratios of the estimated dynamic moduli from P-wave velocities between different directions do not necessarily reflect the actual ratios between elastic constants of the material. In fact, for the anisotropic case, estimating the dynamic elastic modulus from traditional ultrasonic P-wave testing alone can be considered unreliable.

Comparing the dynamic Young's modulus evaluated from IEV testing with that evaluated from UPV testing with P-waves across the length of the specimens can be considered a more robust way of evaluating the reliability of the results from UPV testing. In theory, the stresses developed during testing with these two methods should be resisted across the same material direction as illustrated in Figure 12.

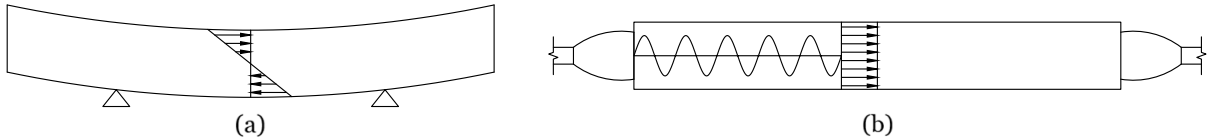(a)   (b)

Figure 12: Schematic representation of (a) stresses in material during flexural IEV test, (b) stresses in material during UPV testing across length.

Table 6 presents the relative scatter between E_{IEV} and $E_{UPV,L}$ for each specimen group.

Table 6: Comparison of dynamic Young's modulus from IEV and UPV measured across length.

Specimen Group	No. of specimens tested	Average values				
		E_{IEV} [MPa]	coeff. of variation	$E_{UPV,L}$ [MPa]	coeff. of variation	$\frac{E_{IEV}-E_{UPV,L}}{E_{IEV}}$
35				Units		
I(a)	7	7,882	15%	7,837	18%	1%
I(b)	6	7,931	17%	7,938	13%	-0.1%
II	5	18,313	1%	13,756	4%	**25%**
III	3	7,107	13%	7,305	2%	-3%
IV	6	15,505	1%	9,157	8%	**41%**
V(a)	2	5,475	8%	5,498	4%	-0.4%
V(b)	6	4,068	30%	4,604	35%	-13%
21				Mortar		
MB	5	3,987	10%	4,527	6%	-14%
MIIB	8	4,269	6%	4,887	16%	-14%
MC	8	28,954	5%	28,601	4%	1%

From Table 6, it is clear that the differences between E_{IEV} and $E_{UPV,L}$ are significantly greater for specimens from group II and IV when compared to the differences for specimens from any other group of constituent materials tested. This suggests that values of dynamic Young's modulus evaluated from UPV testing only with P-waves is unreliable for bricks produced by extrusion due to their apparent anisotropy. Hence, the comparison of E_{IEV} and $E_{UPV,L}$ has brought us to the same conclusion as the comparison of the dynamic Young's moduli estimated from ultrasonic compression wave velocities across different directions. However, in this case, the disagreement between E_{IEV} and $E_{UPV,L}$ is much more apparent and the

comparison does not lend itself to misinterpretation.

From a more general perspective, it is clear that the bricks manufactured through an extrusion process (groups II and IV) show the smallest coefficients of variation. As previously discussed, one of the main reasons for this is that they are characterised by greater homogeneity.

For results from IEV testing, the estimates of dynamic Poisson's ratio generally have greater coefficients of variation, indicating that the evaluation of this parameter is more sensitive to heterogeneities and to changes in testing conditions (see Table 3). Nevertheless, for specimens characterised by a more marked isotropic behaviour, it can be said that IEV testing can provide reliable estimates of the dynamic Poisson's ratio. In fact, most specimen groups have a coefficient of variation of 31% or less for this parameter with the exception of groups I(b) and V(b). Even so, it should be noted that the average estimated value of the dynamic Poisson's ratio was quite low for both these groups of specimens. Hence, the 41% and 70% coefficients of variation among specimens from group I(b)and V(b) respectively, relate to variations of only 0.04 and 0.02 respectively in the estimated Poisson's ratio. The value of the dynamic Poisson's ratio determined for the cement mortar is significantly higher than that of the lime mortar and of the brick specimens handmade in moulds.

One of the main advantages of being able to determine the dynamic Poisson's ratio reliably using IEV testing, is that it can provide a value for a previously unknown parameter in Equation (3), used to compute the dynamic Young's modulus from the experimentally evaluated ultrasonic compression wave velocity. In order to evaluate the benefit gained from this information, a sensitivity study was carried out between the assumed dynamic Poisson's ratio and the evaluated dynamic Young's modulus for all brick specimens. If no information is known on the dynamic Poisson's ratio, it can be assumed that this value can fall anywhere within the range of values determined from IEV testing across all brick specimens tested as part of this research. Hence, the sensitivity study includes Poisson's ratios ranging from 0.01 to 0.37. The results of this study for $E_{UPV,L}$ are shown first only for bricks from group I(a) (Figure 13) and subsequently for all brick specimen groups (Figure 14).
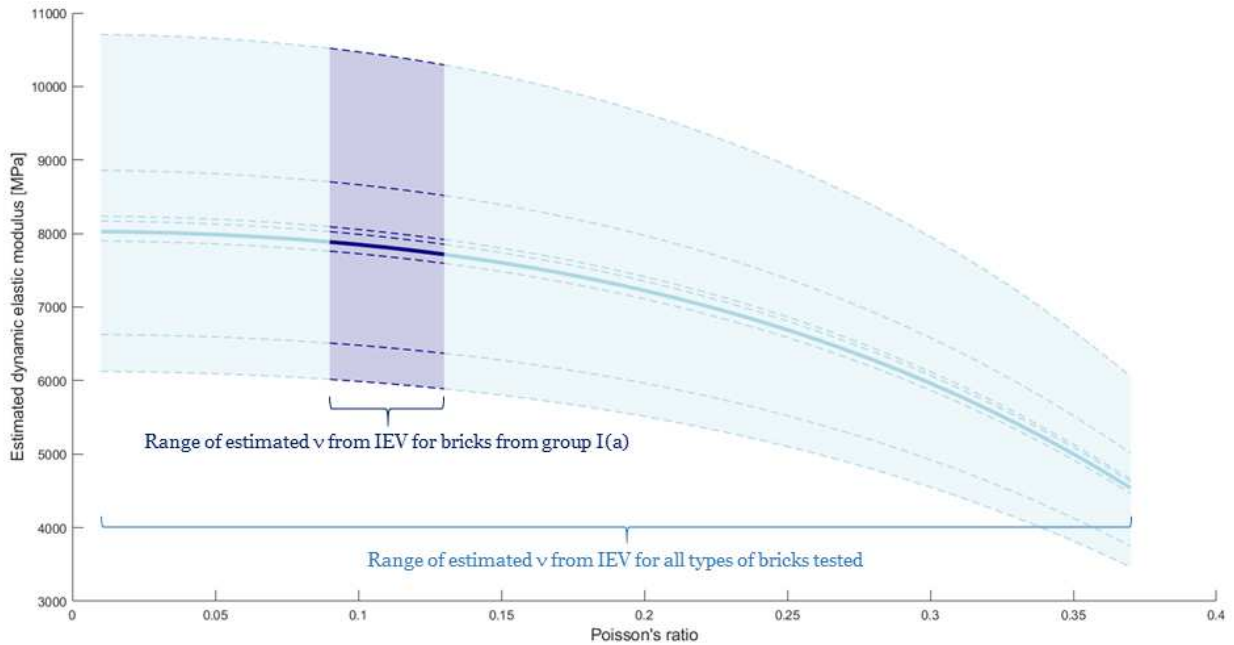

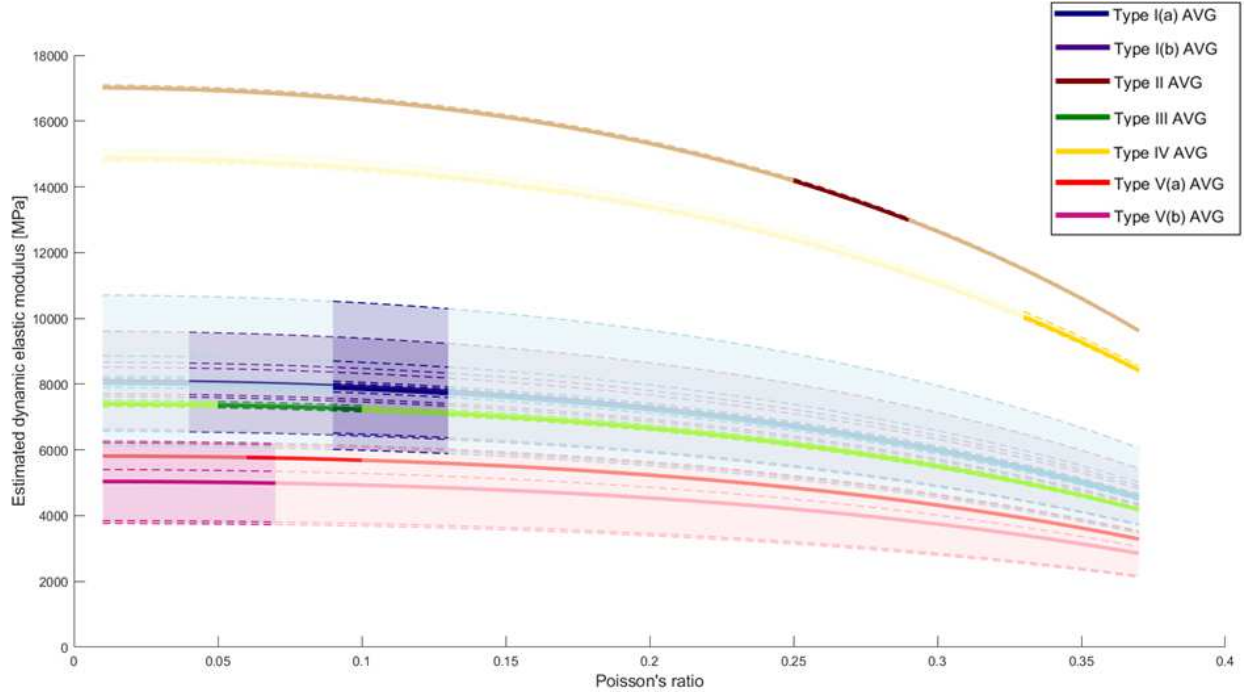Figure 13: Variation of estimation of $E_{UPV,L}$ with ν for bricks from group I(a).

17

Figure 14: Variation of estimation of $E_{UPV,L}$ with ν for all bricks tested as part of this experimental campaign. Areas shaded with a lighter colour refer to the range of estimated ν across all the types of bricks tested. Areas shaded with a darker colour refer to the range of estimated ν for a specific group.(For interpretation of the references to colour in this figure, the reader is referred to the web version of this article.)

A similar trend across an equivalent range of values as shown for $E_{UPV,L}$ was observed for the sensitivity studies of $E_{UPV,W}$ and $E_{UPV,T}$. It is clear to see that using the information on the dynamic Poisson's ratio obtained from IEV testing can contribute to a significant improvement in the estimation of the dynamic Young's modulus from UPV testing. In fact, the sensitivity study revealed that using the Poisson's ratios only within the range estimated from IEV testing for each specific brick specimen group reduced the maximum variation in the estimated dynamic Young's modulus from 50% to a maximum of 3.6%.

It should be noted that although the coefficients of variation for the computed Poisson's ratio are lowest for the bricks produced by extrusion (see Table 3), the estimated values of this parameter for these types of bricks are unreliable. The main reason for this is that bricks manufactured from an extrusion process usually exhibit a certain level of anisotropy. As previously discussed, results from the tests carried out as part of this research confirm this anisotropic character. Since a fundamental assumption behind the analytical expression used for the computation of Poisson's ratio from IEV results is isotropy, these values cannot be considered reliable estimates. Nevertheless, the values of dynamic shear modulus evaluated from the torsional IEV tests do not depend on Poisson's ratio and therefore still provide a good representation of how the material behaves in the orientation in which it was tested. Although the expression relating the measured flexural resonant frequency to the dynamic Young's modulus (Equation (1)) contains a correction factor dependent on Poisson's ratio, the final estimated value is very insensitive to changes in Poisson's ratio. In fact, a simple sensitivity study showed that this parameter has a maximum variation of less than 1.74% for any specimen over the whole range of estimated Poisson's ratios across all specimen groups. Hence, it can be said that IEV testing also provides a good representation of the dynamic Young's modulus of anisotropic bricks when acting against out-of-plane flexural loads.

5. Proposed analysis procedure

Based on all the experimental methods described in detail in Sections 3.2 and 3.3, a summary of the recommended analysis procedure for obtaining reliable estimates of the dynamic elastic properties of brick masonry constituents is shown in Figure 15.
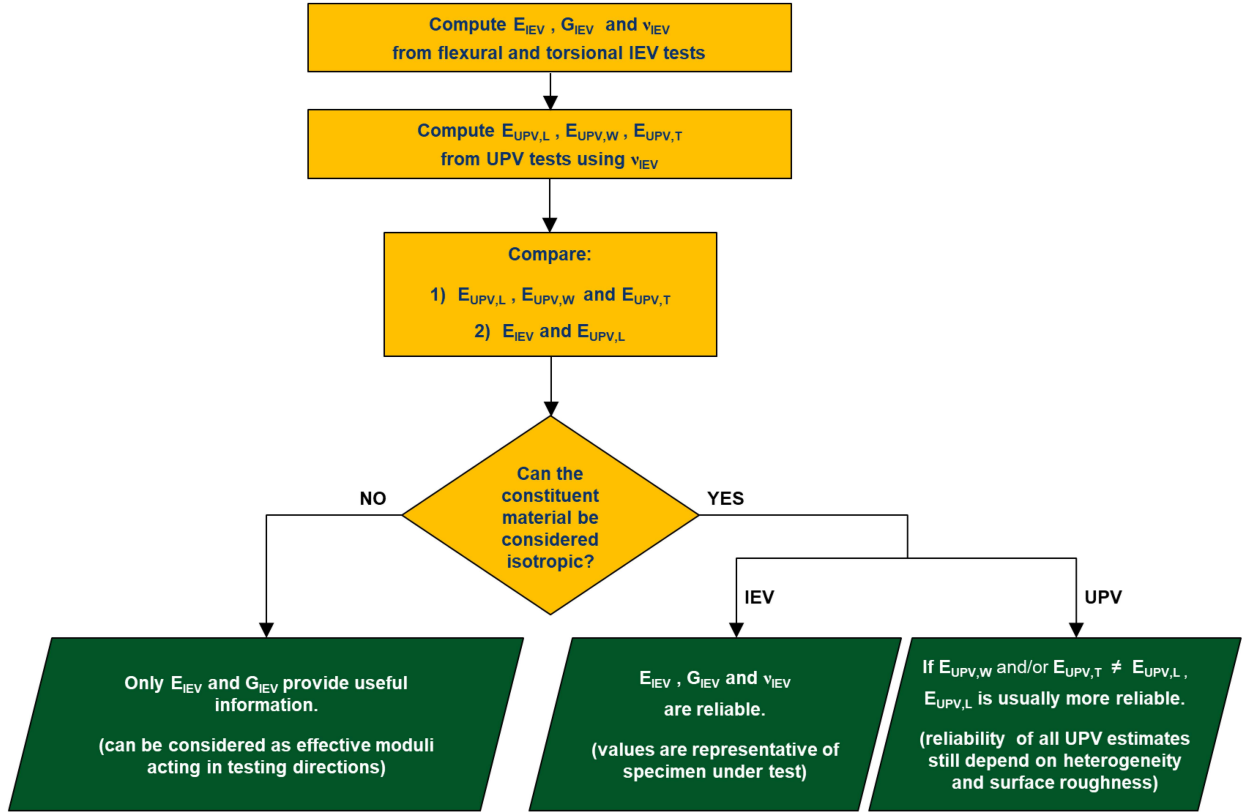
18

Figure 15: Summary of the proposed procedure for determining dynamic elastic properties of brick masonry constituents.

As can be seen from Figure 15, the first step of the analysis process involves computing E_{IEV}, G_{IEV} and ν_{IEV} from the results of IEV tests conducted as described in Section 3.2. Following this, the resulting ν_{IEV} is used in the computation of $E_{UPV,L}$, $E_{UPV,W}$ and $E_{UPV,T}$ from ultrasonic pulse velocities measured across different dimensions of each specimen as described in Section 3.3. The average values for each group of specimens representing a particular type of brick or mortar can then be obtained. All subsequent analysis can be carried out with these representative average values. Once these values have been obtained, it is important to assess if any of the brick or mortar types being tested exhibit a significant level of anisotropy in order to evaluate the reliability of the obtained results. If there are significant relative scatters (>30%) between $E_{UPV,L}$, $E_{UPV,W}$ and $E_{UPV,T}$ as well as a significant relative scatter (>20%) between E_{IEV} and $E_{UPV,L}$ then the type of brick or mortar under test can be said to be anisotropic. If this is the case, only the dynamic Young's modulus (E_{IEV}) and the dynamic shear modulus (G_{IEV}) computed from results of IEV testing provide a good representation of the behaviour of the material in the respective testing orientations. On the other hand, if the material exhibits a predominantly isotropic behaviour, in theory, all the dynamic elastic material properties evaluated from IEV and UPV testing can be considered reliable. However, since the reliability of UPV estimates depend strongly on heterogeneity and surface roughness, if $E_{UPV,W}$ and/or $E_{UPV,T}$ differ from $E_{UPV,L}$, the latter parameter can be considered as being more reliable in most cases.

The application of this analysis process can be illustrated with two simple examples. Taking the case of the cement mortar tested as part of this research (group MC), the relative scatters between $E_{UPV,L}$, $E_{UPV,W}$ and $E_{UPV,T}$ are all of 5% or less and the relative scatter between E_{IEV} and $E_{UPV,L}$ is of only 1%. In this case, it is clear that the material is isotropic and all the estimated dynamic elastic properties can be considered reliable. On the contrary, for the type of bricks belonging to group II, the relative scatter between $E_{UPV,L}$ and $E_{UPV,T}$ is 35% while that between $E_{UPV,W}$ and $E_{UPV,T}$ is 46%. Furthermore, the relative scatter between E_{IEV} and $E_{UPV,L}$ turned out to be 25%. For these bricks, all properties estimated from UPV tests as well as the value of ν_{IEV} cannot be considered reliable. Nevertheless, E_{IEV} is still representative of the dynamic Young's modulus when out-of-plane flexural loads are acting on this type of brick while G_{IEV} still provides a good representation of the response of bricks of this type to torsional loads (in the same orientation as the bricks were tested).

6. Conclusions and future work

The research has proposed a robust procedure based on the synergy of two approaches, namely Impulse Excitation of Vibration (IEV) and Ultrasonic Pulse Velocity (UPV) testing for the determination of the dynamic elastic properties of brick masonry constituents. The influence of testing conditions and other factors specific to brick masonry constituents have been evaluated to assess the applicability of these techniques. At the same time, methods to mitigate possible sources of error have been explored and as a result, clear practical provisions have been given concerning every step of the procedure from testing protocols to the interpretation of results. Moreover, in order to derive meaningful ranges of results for different masonry typologies, the experimental program has explored different types of bricks and mortars. The tests have considered hydraulic lime mortar, cement mortar, new bricks manufactured using either hand-made moulding or extrusion, and existing bricks extracted from heritage buildings in Barcelona, Spain.

The proposed methodology can be applied to whole brick specimens as well as to specifically-cast mortar specimens. In the case of whole brick specimens, these can be recently manufactured or extracted from existing constructions. In the latter scenario, the methods described in this paper cannot be considered as being fully non-destructive since they implicitly require the extraction of bricks from the structure. Nevertheless, both methods can be used to test extracted bricks without causing any further significant damage to the material, allowing the same bricks to be re-used or to undergo further testing. In the case of mortar specimens, since they have to be cast to specific dimensions, the proposed testing procedures are not suitable for testing mortar already present in existing masonry structures. Nevertheless, the procedures can be applied to test freshly-cast mortar either for use in new constructions or intended for repair works. The results obtained from the present investigation show that the two methods (IEV and UPV) can provide reliable estimates of the actual dynamic elastic properties of typical brick masonry constituents.

For isotropic constituent materials, one of the main advantages of the proposed procedure lies in using the dynamic Poisson's ratio derived from IEV tests to improve the accuracy of the dynamic Young's modulus evaluated from conventional UPV tests based on the transmission of P-waves. Since UPV tests are simpler and faster to execute when compared to IEV tests, a possible application of this procedure could involve determination of the dynamic Poisson's ratio using IEV testing on a selected number of specimens together with characterisation of the dynamic Young's modulus using UPV testing on a larger sample size. In the case of existing single-leaf walls, this procedure may even be extended to in situ UPV tests on bricks.

The results reveal that bricks produced by a conventional extrusion procedure exhibit a significant level of anisotropy. In this case, the estimation of the dynamic Young's modulus from traditional UPV tests is not reliable since the propagation of ultrasonic waves is not governed by the same simplified rules as in isotropic media. The procedure involving the combined information from flexural and torsional IEV tests to evaluate the dynamic Poisson's ratio is also not applicable to such bricks since it relies on the fundamental assumption of isotropy. Nevertheless, IEV tests can still provide estimates of effective dynamic elastic moduli which define the behaviour of brick specimens when subjected to flexural or torsional loading.

An extension of the research presented herein may explore testing procedures involving ultrasonic shear wave transducers to better characterise the dynamic elastic behaviour of anisotropic bricks. Theoretically, such transducers could also be used to directly evaluate the dynamic Poisson's ratio of isotropic constituents. However, it should be noted that accurately determining the arrival time of the shear wave can prove to be especially difficult, particularly when testing brick-sized specimens of materials with significant heterogeneities and rough surfaces.

One of the most important implications of this work is that it provides a means of better understanding the relationship between static and dynamic elastic properties for brick masonry constituents. This relationship is as of yet not well understood. Additional laboratory investigations are currently being carried out at the Universitat Politècnica de Catalunya to correlate the static and dynamic elastic properties in different masonry components.
.

Conflicts of interest

The authors confirm that there are no known conflicts of interest associated with this publication.

Acknowledgements

References

[1] European Committee for Standardization (CEN), EN 14580:2005. Natural stone test methods - Determination of static elastic modulus (2005).

[2] L. Binda, C. Tiraboschi, G. Mirabella Roberti, G. Baronio, G. Cardani, Measuring masonry material properties: detailed results from an extensive experimental research Part I: Tests on masonry components. (Report 5.1 Politecnico di Milano)., Tech. rep., Politecnico di Milano (1996).

[3] L. Binda, C. Tiraboschi, S. Abbaneo, Experimental Research to Characterise Masonry Materials, Masonry International. URL https://www.masonry.org.uk/downloads/experimental-research-to-characterise-masonry-materials/

[4] L. Binda, C. Tedeschi, P. Condoleo, Characterisation of Materials Sampled From Some My S'on Temples, in: 7th International Congress on Civil Engineering, 2006.

[5] G. Baronio, L. Binda, C. Tedeschi, C. Tiraboschi, Characterisation of the materials used in the construction of the Noto Cathedral, Construction and Building Materials 17 (8) (2003) 557–571. doi:10.1016/j.conbuildmat.2003.08.007.

[6] D. V. Oliveira, Mechanical Characterization of Stone and Brick Masonry (Report 00-DEC/E-4), Tech. rep., University of Minho (2000).

[7] D. V. Oliveira, P. B. Lourenço, P. Roca, Experimental Characterization of the Behaviour of Brick Masonry Subjected to Cyclic Loading, in: 12th international Brick/Block Masonry Conference, no. May 2014, 2000, pp. 1–8.

[8] D. V. Oliveira, P. B. Lourenço, P. Roca, Cyclic behaviour of stone and brick masonry under uniaxial compressive loading, Materials and Structures/Materiaux et Constructions 39 (286) (2006) 247–257. doi:10.1617/s11527-005-9050-3.

[9] L. Pelà, E. Canella, A. Aprile, P. Roca, Compression test of masonry core samples extracted from existing brickwork, Construction and Building Materials 119 (2016) 230–240. doi:10.1016/j.conbuildmat.2016.05.057.

[10] E. I. Mashinsky, Differences between static and dynamic elastic moduli of rocks: Physical causes, Russian Geology and Geophysics 44 (9) (2003) 953–959.

[11] M. Ciccotti, F. Mulargia, Differences between static and dynamic elastic moduli of a typical seismogenic rock, Geophysical Journal International 157 (1) (2004) 474 – 477.

[12] J. Martínez-Martínez, D. Benavente, M. A. García-del Cura, Comparison of the static and dynamic elastic modulus in carbonate rocks, Bulletin of Engineering Geology and the Environment 71 (2) (2012) 263–268. doi:10.1007/s10064-011-0399-y.

[13] A. R. Najibi, M. Ghafoori, G. R. Lashkaripour, M. R. Asef, Empirical relations between strength and static and dynamic elastic properties of Asmari and Sarvak limestones, two main oil reservoirs in Iran, Journal of Petroleum Science and Engineering 126 (2015) 78–82. doi:10.1016/j.petrol.2014.12.010. URL http://dx.doi.org/10.1016/j.petrol.2014.12.010

[14] W. Fei, B. Huiyuan, Y. Jun, Z. Yonghao, Correlation of Dynamic and Static Elastic Parameters of Rock, Electronic Journal of Geotechnical Engineering 21 (04) (2016) 1551–1560.

[15] Y. Z. Totoev, J. M. Nichols, A Comparative Experimental Study of the Modulus of Elasticity of Bricks and Masonry, in: 11th International Brick/Block Masonry Conference, no. October, 1997.

[16] J. M. Nichols, Y. Z. Totoev, Experimental determination of the dynamic Modulus of Elasticity of masonry units, in: 15th Australian Conference on the Mechanics of Structures and Materials (ACMSM), 1997.

[17] ASTM, E 1876 - Standard Test Method for Dynamic Young's Modulus, Shear Modulus, and Poisson's Ratio by Impulse Excitation of Vibration (2002). doi:10.1520/E1876-09.responsibility.

[18] ASTM, C597 - Standard Test Method for Pulse Velocity Through Concrete (2010). `doi:10.1520/C0597-09`.

[19] V. Brotons, R. Tomás, S. Ivorra, A. Grediaga, Relationship between static and dynamic elastic modulus of calcarenite heated at different temperatures: The San Julián's stone, Bulletin of Engineering Geology and the Environment 73 (3) (2014) 791–799. `doi:10.1007/s10064-014-0583-y`.

[20] S. Dimter, T. Rukavina, K. Minažek, Estimation of elastic properties of fly ash-stabilized mixes using nondestructive evaluation methods, Construction and Building Materials 102 (2016) 505–514. `doi:10.1016/j.conbuildmat.2015.10.175`.

[21] M. Asmani, C. Kermel, A. Leriche, M. Ourak, Influence of porosity on Youngs modulus and poisson's ratio in alumina ceramics, Journal of the European Ceramic Society 21 (8) (2001) 1081–1086. `doi:10.1016/S0955-2219(00)00314-9`.

[22] L. E. García, Estudio experimental del comportamiento a compresión de elementos pétreos confinados con materiales compuestos, Doctoral thesis, Universitat d'Alacant (2018).

[23] J. D. Achenbach, Wave propagation in elastic solids, Vol. 16, 1973. `arXiv:arXiv:1011.1669v3, doi:10.1002/zamm.19920720607`.

[24] P. Laugier, G. Haïat, Chapter 2: Introduction to the Physics of Ultrasound, in: Bone Quantitative Ultrasound, 2011, pp. 29–45. `arXiv:arXiv:1011.1669v3, doi:10.1007/978-94-007-0017-8`.

[25] J. H. Bungey, S. G. Millard, M. G. Grantham, Testing of Concrete in Structures, 1996.

[26] Z. Nazarchuk, V. Skalskyi, O. Serhiyenko, Chapter 2: Propagation of Elastic Waves in Solids, in: Acoustic Emission, Vol. i, Springer International Publishing, 2017, pp. 29–73. `doi:10.1007/978-3-319-49350-3`.
URL `http://link.springer.com/10.1007/978-3-319-49350-3`

[27] C. Lane, Wave Propagation in Anisotropic Media, in: The Development of a 2D Ultrasonic Array Inspection for Single Crystal Turbine Blades, 2014, pp. 13–39. `doi:10.1007/978-3-319-02517-9_2`.
URL `http://link.springer.com/10.1007/978-3-319-02517-9{_}2`

[28] J. L. Rose, Ultrasonic Guided Waves in Solid Media, Cambridge University Press, New York, 2014. `doi:10.1017/CBO9781107273610`.
URL `http://ebooks.cambridge.org/ref/id/CBO9781107273610`

[29] J. L. Rose, Ultrasonic Waves in Solid Media, Cambridge University Press, 1999.

[30] European Committee for Standardization (CEN), EN 12504-4:2004. Testing concrete Part 4: Determination of ultrasonic pulse velocity (2004). `doi:ConstructionStandard,CS1:2010`.

[31] A. Fódi, Effects influencing the compressive strength of a solid, fired clay brick, Periodica Polytechnica Civil Engineering 55 (2) (2011) 117–128. `doi:10.3311/pp.ci.2011-2.04`.

[32] European Committee for Standardization (CEN), EN 771-1:2011+A1:2015. Specification for masonry units Part 1: Clay masonry units (2015).

[33] European Committee for Standardization (CEN), EN 772-1. Methods of test for masonry units. Part 1: Determination of compressive strength (2010).

[34] European Committee for Standardization (CEN), EN 1015-11. Methods of test for mortar for masonry - Part 11: Determination of flexural and compressive strength of hardened mortar (2007).

[35] National Instruments, LabVIEW 2016 Help (2016).

[36] ASTM, C 1259 - Standard Test Method for Dynamic Young 's Modulus , Shear Modulus , and Poisson's Ratio for Advanced Ceramics by Impulse Excitation of Vibration (2001). `doi:10.1520/E1875-08.2`.

[37] MathWorks, MATLAB R2017b Documentation.
URL `https://es.mathworks.com/help/releases/R2017b/index.html`

[38] M. Farshchin, Frequency Domain Decomposition (FDD) (2015).

[39] PROCEQ, PUNDIT PL-200 Operating Instructions (2014).